Gas Dynamics and Heat and Mass Transfer

Fractional Step Method

Student: Pedro López Sancha

Professor: Carlos-David Pérez Segarra

Aerospace Technology Engineering
The School of Industrial, Aerospace and Audiovisual Engineering of Terrassa
Technic University of Catalonia

March 4, 2022

UNIVERSITAT POLITÈCNICA DE CATALUNYA
BARCELONATECH

Escola Superior d'Enginyeries Industrial,
Aeroespacial i Audiovisual de Terrassa

Contents

Chapter 1

Theoretical background

Theorem 1.0.1 (Helmholtz–Hodge FSM)**.** Let $\Omega \subset \mathbb{R}^3$ be a bounded domain with smooth boundary. Let $\boldsymbol{\omega}\colon \Omega \subset \mathbb{R}^3 \to \mathbb{R}^3$ be a vector field. Then there exist a smooth function $\varphi\colon \Omega \subset \mathbb{R}^3 \to \mathbb{R}$ and a divergence-less smooth vector field $\mathbf{a}\colon \Omega \subset \mathbb{R}^3 \to \mathbb{R}^3$ such that

$$\boldsymbol{\omega} = \mathbf{a} + \boldsymbol{\nabla}\varphi$$

In addition,

$$\mathbf{a} \cdot \boldsymbol{\nu} = 0 \quad \text{on } \partial\Omega$$

where $\boldsymbol{\nu}$ denotes the outer normal vector to $\partial\Omega$.

Theorem 1.0.2 (Helmholtz–Hodge)**.** Let $D \subset \mathbb{R}^3$ be a bounded domain. Then every smooth vector field $\mathbf{F}\colon D \to \mathbb{R}^3$ can be decomposed into a sum $\mathbf{F} = \mathbf{F}_1 + \mathbf{F}_2$, where $\mathbf{F}_1$ is an irrotational field and $\mathbf{F}_2$ is a solenoidal field.

Theorem 1.0.3 (Helmholtz–Hodge)**.** Let $\Omega \subset \mathbb{R}^3$ be a contractible bounded open set with smooth boundary. Let $F\colon \Omega \subset \mathbb{R}^3 \to \mathbb{R}^3$ be a $\mathcal{C}^\infty(\Omega)$ vector field. Then there exist a function $f \in \mathcal{C}^\infty(\Omega, \mathbb{R})$ and a vector field $H \in \mathcal{C}^\infty(\Omega, \mathbb{R}^3)$ such that

$$F = \boldsymbol{\nabla} f + \boldsymbol{\nabla} \times H$$

Theorem 1.0.4. Let $\Omega \subset \mathbb{R}^3$ be a contractible bounded open set with smooth boundary. Let $G\colon \Omega \subset \mathbb{R}^3 \to \mathbb{R}^3$ be a divergence–free $\mathcal{C}^\infty(\Omega)$ vector field, that is to say, $\boldsymbol{\nabla} \cdot G = 0$. Then there exists a $\mathcal{C}^\infty(\Omega)$ vector field $g\colon \Omega \subset \mathbb{R}^3 \to \mathbb{R}^3$ such that $\boldsymbol{\nabla} \times g = G$.

Notice that the previous theorem says nothing about the uniqueness of the field g.

Assume F is the Schwartz space

Then see Griffith's of Helmholtz's theorem

Chapter 2

Fractional Step Method

In this Chapter the Fractional Step Method (FSM) is introduced and justified. asdsadas

Hereinafter, it is assumed that the studied PDEs occur in a bounded open set $\Omega \subset \mathbb{R}^3$ with boundary as smooth as necessary, and last for finite time, that is to say, the time interval is $I = (0, t_{\max}) \subset \mathbb{R}$ with $t_{\max} > 0$.

2.1 First approach to the FSM

2.1.1 Time integration of the Navier–Stokes equations

Recall that the Navier–Stokes equations for incompressible and constant viscosity flows are given by

$$\begin{cases} \boldsymbol{\nabla} \cdot \mathbf{v} = 0 \\ \rho \dfrac{\partial \mathbf{v}}{\partial t} + (\rho \mathbf{v} \cdot \boldsymbol{\nabla}) \mathbf{v} = -\boldsymbol{\nabla} p + \mu \boldsymbol{\Delta} \mathbf{v} \end{cases} \tag{2.1}$$

where ρ and μ are the fluid density and viscosity, respectively, $p \colon \Omega \times I \to \mathbb{R}$ is the pressure field and $\mathbf{v} = (u, v, w) \colon \Omega \times I \to \mathbb{R}^3$ is the velocity field. The operator

$$\mathbf{R}(t, \mathbf{v}) = \mu \boldsymbol{\Delta} \mathbf{v}(\cdot, t) - (\rho \mathbf{v}(\cdot, t) \cdot \boldsymbol{\nabla}) \mathbf{v}(\cdot, t) = \mu \boldsymbol{\Delta} \mathbf{v} - (\rho \mathbf{v} \cdot \boldsymbol{\nabla}) \mathbf{v} \tag{2.2}$$

permits rewriting Equation (2.1) as follows:

$$\begin{cases} \boldsymbol{\nabla} \cdot \mathbf{v} = 0 \\ \rho \dfrac{\partial \mathbf{v}}{\partial t} = \mathbf{R}(t, \mathbf{v}) - \boldsymbol{\nabla} p \end{cases} \tag{2.3}$$

Therefore the momentum equation is now an evolution equation.

In order to solve (2.3) numerically in $\Omega \times I \subset \mathbb{R}^4$ with suitable boundary conditions on $\partial\Omega$ and initial conditions on $\Omega \times \{t = 0\}$ following a finite volume method, it is necessary to discretise Ω in control volumes and integrate (2.3) over time intervals of the form $[t^n, t^{n+1}]$.

Let $[t^n, t^{n+1}] \subset [t_0, t_f] = \overline{I}$ be a non–degenerate time interval and $\Delta t = t^{n+1} - t^n$. An implicit integration scheme ($\beta = 1$) is used to integrate the continuity equation with respect to time:

$$\int_{t^n}^{t^{n+1}} \boldsymbol{\nabla} \cdot \mathbf{v} \, \mathrm{d}t = \left(\beta (\boldsymbol{\nabla} \cdot \mathbf{v})^{n+1} + (1 - \beta)(\boldsymbol{\nabla} \cdot \mathbf{v})^n \right) \Delta t = (\boldsymbol{\nabla} \cdot \mathbf{v})^{n+1} \, \Delta t = 0$$

Since $\Delta t > 0$, it follows that

$$(\boldsymbol{\nabla} \cdot \mathbf{v})^{n+1} \approx \boldsymbol{\nabla} \cdot \mathbf{v}^{n+1} = 0 \tag{2.4}$$

which is the time–integrated continuity equation. As for the momentum equation,

$$\int_{t^n}^{t^{n+1}} \rho \frac{\partial \mathbf{v}}{\partial t} \, \mathrm{d}t = \int_{t^n}^{t^{n+1}} \mathbf{R}(\mathbf{v}) \, \mathrm{d}t - \int_{t^n}^{t^{n+1}} \boldsymbol{\nabla} p \, \mathrm{d}t$$

For the left–hand side, it is known that the density is constant, hence:

$$\int_{t^n}^{t^{n+1}} \rho \frac{\partial \mathbf{v}}{\partial t} \, \mathrm{d}t = \rho \int_{t^n}^{t^{n+1}} \frac{\partial \mathbf{v}}{\partial t} \, \mathrm{d}t = \rho(\mathbf{v}^{n+1} - \mathbf{v}^n)$$

In order to integrate $\mathbf{R}(\mathbf{v})$, define

$$\mathfrak{R}(t, \mathbf{v}) = \int_0^t \mathbf{R}(s, \mathbf{v}) \, \mathrm{d}s$$

so that

$$\mathfrak{R}(t^{n+1}, \mathbf{v}) - \mathfrak{R}(t^n, \mathbf{v}) = \int_{t^n}^{t^{n+1}} \mathbf{R}(s, \mathbf{v}) \, \mathrm{d}s \tag{2.5}$$

By applying the two–step Adams–Bashforth method, (2.5) results in

$$\int_{t^n}^{t^{n+1}} \mathbf{R}(s, \mathbf{v}) \, \mathrm{d}t = \left(\frac{3}{2} \mathbf{R}(t^n, \mathbf{v}) - \frac{1}{2} \mathbf{R}(t^{n-1}, \mathbf{v}) \right) \Delta t$$

For the sake of simplicity in notation, it shall be written $\mathbf{R}(\mathbf{v}^n)$ in place of $\mathbf{R}(t^n, \mathbf{v})$. Regarding the integral of the pressure gradient, again the implicit integration scheme ($\beta = 1$) is used, which yields

$$\int_{t^n}^{t^{n+}} \boldsymbol{\nabla} p \, \mathrm{d}t = \left(\beta \boldsymbol{\nabla} p^{n+1} + (1 - \beta) \boldsymbol{\nabla} p^n \right) \Delta t = \boldsymbol{\nabla} p^{n+1} \, \Delta t$$

By rearranging terms the time–integrated momentum equation is obtained:

$$\rho \frac{\mathbf{v}^{n+1} - \mathbf{v}^n}{\Delta t} = \frac{3}{2} \mathbf{R}(\mathbf{v}^n) - \frac{1}{2} \mathbf{R}(\mathbf{v}^{n-1}) - \boldsymbol{\nabla} p^{n+1} \tag{2.6}$$

2.1.2 Application of the Helmholtz decomposition to the Navier–Stokes equations

Define the predictor velocity by

$$\mathbf{v}^p = \mathbf{v}^{n+1} + \frac{\Delta t}{\rho} \boldsymbol{\nabla} p^{n+1} \tag{2.7}$$

Since the velocity field is divergence–less, the predictor velocity is decomposed into... which is unique

After introducing (2.7) into (2.6), the time–integrated momentum equation becomes the velocity projection equation:

$$\rho \frac{\mathbf{v}^p - \mathbf{v}^n}{\Delta t} = \frac{3}{2} \mathbf{R}(\mathbf{v}^n) - \frac{1}{2} \mathbf{R}(\mathbf{v}^{n-1}) \tag{2.8}$$

Taking the divergence of both sides of (2.7) and using (2.4) results in

$$\boldsymbol{\nabla} \cdot \mathbf{v}^p = \boldsymbol{\nabla} \cdot \mathbf{v}^{n+1} + \boldsymbol{\nabla} \cdot \left(\frac{\Delta t}{\rho} \boldsymbol{\nabla} p^{n+1} \right) = \frac{\Delta t}{\rho} \boldsymbol{\Delta} p^{n+1} \tag{2.9}$$

which is a Poisson equation for the pressure term:

$$\boldsymbol{\Delta} p^{n+1} = \frac{\rho}{\Delta t} \boldsymbol{\nabla} \cdot \mathbf{v}^p \tag{2.10}$$

2.1.3 Solving algorithm

Notice that from Equation (2.8) the predictor velocity may also be calculated by

$$\mathbf{v}^p = \mathbf{v}^n + \frac{\Delta t}{\rho}\left(\frac{3}{2}\mathbf{R}(\mathbf{v}^n) - \frac{1}{2}\mathbf{R}(\mathbf{v}^{n-1})\right) \tag{2.11}$$

Assume that the data up to time t^n is known, that is to say, $\mathbf{R}(\mathbf{v}^{n-1}), \mathbf{R}(\mathbf{v}^n)$ and $\mathbf{v}^n$ are known. Then the computation of the predictor velocity is immediate by means of Equation (2.11). By integrating the laplacian of the pressure term at t^{n+1} on each control volume, equation (2.10) may be transformed into a linear equation which, with suitable boundary conditions on $\partial\Omega$, allows us to compute p^{n+1} (this matter is carried out in Section section). As a result, both $\mathbf{v}^p$ and $\boldsymbol{\nabla} p^{n+1}$ are known, whereby the velocity field at t^{n+1} is obtained from Equation (2.7):

$$\mathbf{v}^{n+1} = \mathbf{v}^p - \frac{\Delta t}{\rho}\boldsymbol{\nabla} p^{n+1} \tag{2.12}$$

This procedure is summarised in the following algorithm:

Algorithm 1 Computation of the velocity field at t^{n+1}.

1. Evaluation of $\mathbf{R}(\mathbf{v}^n)$.
2. Evaluation of the predictor velocity $\mathbf{v}^p$ with Equation (2.11).
3. Evaluation of the pressure at t^{n+1} by solving Equation (2.10).
4. Evaluation of the velocity at t^{n+1} with Equation (2.12).

Despite of the simplicity Algorithm 1, the produced velocity and pressure fields entail a fundamental problem, namely, these have no physical meaning. In the section below, an example of this is exposed.

2.2 The checkerboard problem

Consider the x–component of Equation (2.12)

$$u^{n+1} = u^p - \frac{\Delta t}{\rho}\left(\frac{\partial p}{\partial x}\right)^{n+1} \approx u^p - \frac{\Delta t}{\rho}\frac{\partial p^{n+1}}{\partial x} \tag{2.13}$$

and the following discretisation in the x–direction of a neighbourhood of a point P:

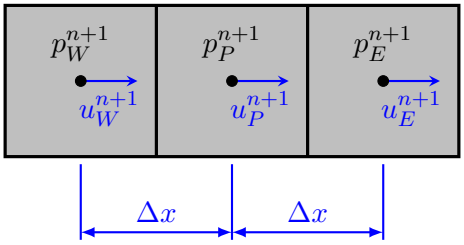

Figure 2.1

By applying finite differences at P to compute the partial derivative in Equation (2.13), one may approximate u_P^{n+1} as follows:

$$u_P^{n+1} = u^p - \frac{\Delta t}{\rho}\frac{p_E^{n+1} - p_W^{n+1}}{2\Delta x} \tag{2.14}$$

We notice that u_P^{n+1} does not depend upon p_P^{n+1}. The same is true for the y and z–components of (2.12). This is a consequence of the pressure p_P^{n+1} and the gradient $\boldsymbol{\nabla} p^{n+1}$ being decoupled, i.e. independent of one another.

This leads to converged velocity fields for unphysical pressure distributions. For instance, consider the following situation

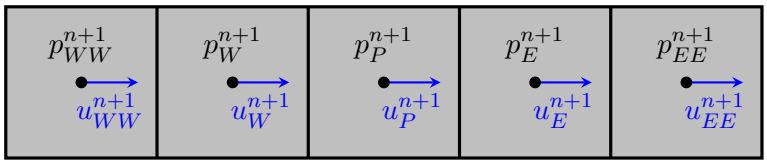

$$p_{WW}^{n+1} = p_P^{n+1} = p_{EE}^{n+1} = 100$$
$$p_W^{n+1} = p_E^{n+1} = 0$$

Figure 2.2

which is a checkerboard pattern as far as the pressure distribution is concerned. The partial derivative of pressure satisfies $\partial_x p^{n+1} = 0$ at nodes W, P and E, despite being a pressure distribution with no physical sense, thus yielding incorrect converged velocities at these nodes. It is clear that a more sophisticated strategy to relate the velocity and pressure fields is needed.

2.3 Second approach to the FSM

2.3.1 Staggered meshes

In order to solve the decoupling of the velocity and pressure fields, two strategies have been developed, namely staggered meshes and collocated meshes. Nonetheless, we shall focus only on the former, more specifically, in the case of cartesian meshes.

In a staggered mesh, rather than locating the pressure and velocity terms at the same point in space as we have done so far, these pressure is set at the centre of the control volume whereas the velocity components are located at the faces of the control volume, as Figure 2.3 shows.

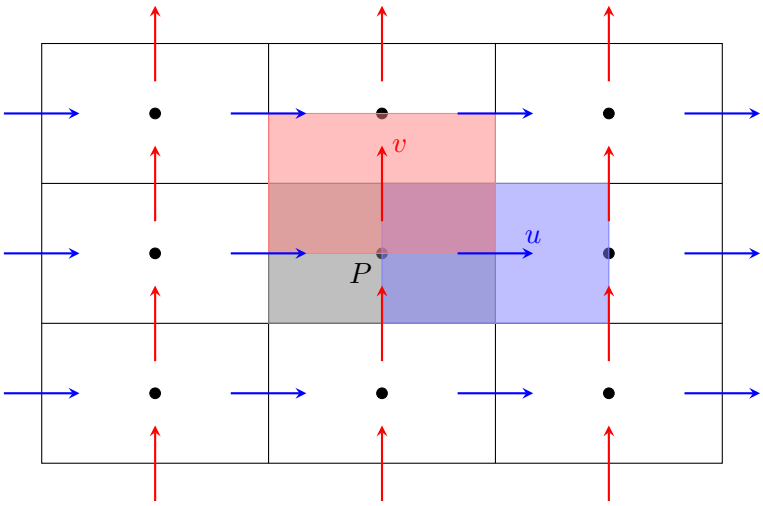

Figure 2.3. Staggered mesh. Source: adapted from asdas

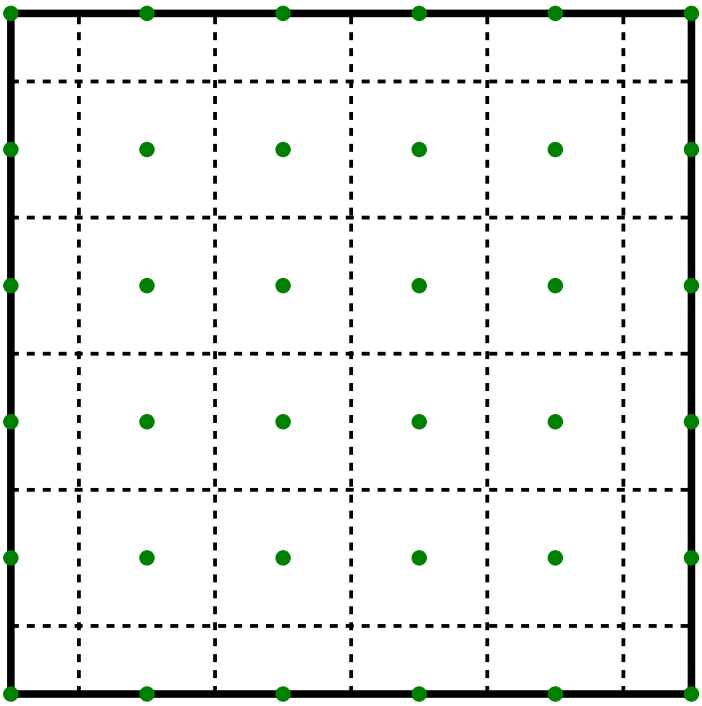

Pressió: cares centrades.

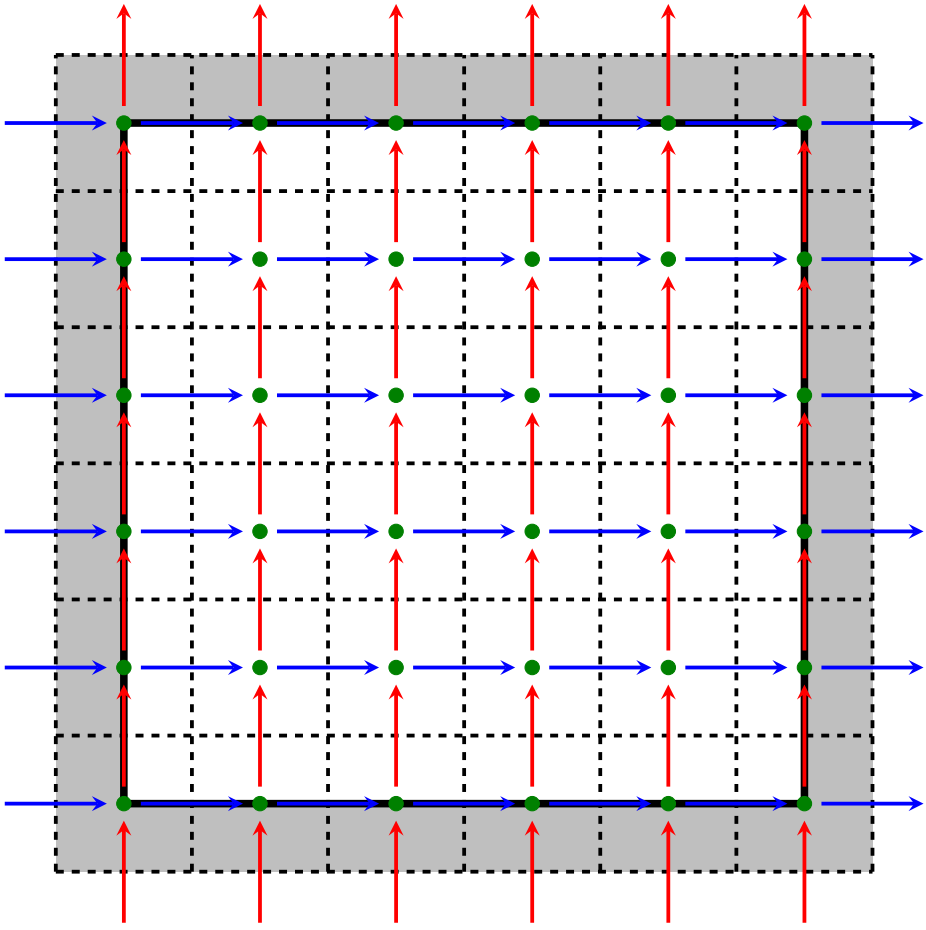

Pressió: cares centrades. Velocitat u: staggered–x. Velocitat v: staggered–y.

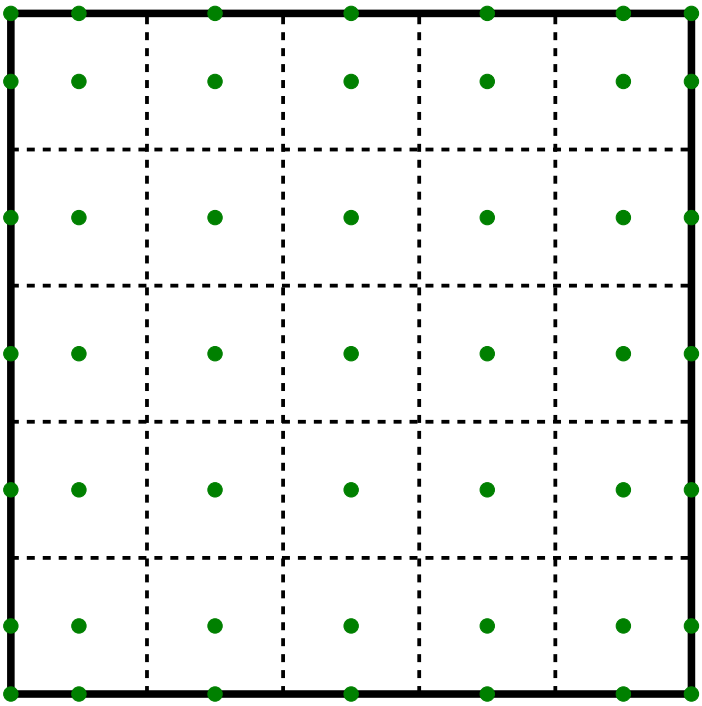

Pressió: nodes centrats.

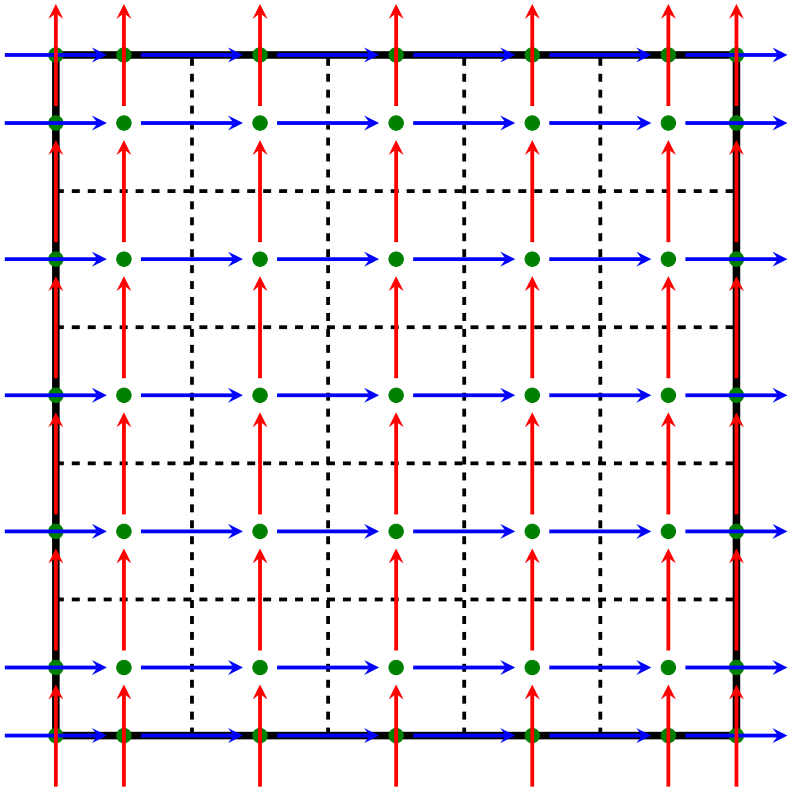

Pressió: nodes centrades. Velocitat u: staggered–x. Velocitat v: staggered–y.

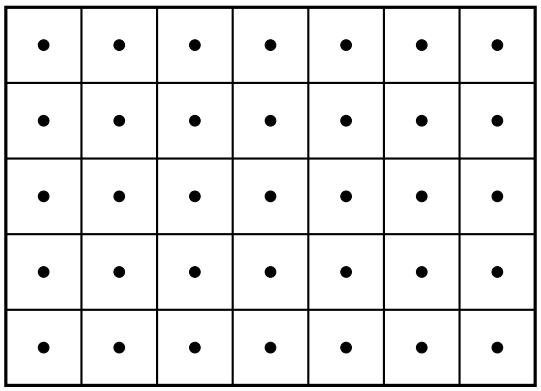

Chapter 3

Lid–Driven Cavity

3.1 Statement

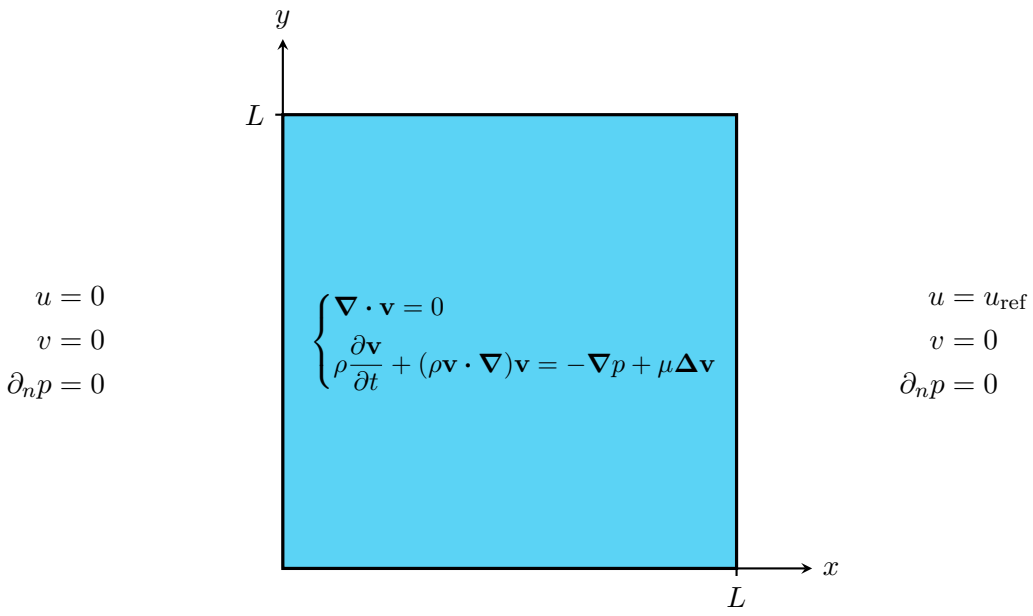

Figure 3.1

$$\int_M \mathrm{d}\omega = \int_{\partial M} \omega$$

asdsadasdasdsadsa

$$\mathcal{B} = \{e_1, \ldots, e_n\}$$